THE JOURNAL OF BIOLOGICAL CHEMISTRY VOL. 288, NO. 8, pp. 5718–5731, February 22, 2013

Selective Inhibition of Phosphoinositide 3-Kinase p110α Preserves Lymphocyte Function*

Received for publication, September 28, 2012, and in revised form, December 20, 2012 Published, JBC Papers in Press, December 28, 2012, DOI 10.1074/jbc.M112.379446

Lomon So[‡], Sung Su Yea[‡§], Jean S. Oak[‡], Mengrou Lu[‡], Arun Manmadhan[‡], Qiao Han Ke[‡], Matthew R. Janes[¶‖], Linda V. Kessler[¶‖], Jeff M. Kucharski[¶‖], Lian-Sheng Li[¶‖], Michael B. Martin[¶‖], Pingda Ren[¶], Katti A. Jessen[¶‖], Yi Liu[¶], Christian Rommel[¶], and David A. Fruman[‡1]

From the [‡]Department of Molecular Biology & Biochemistry, and Institute for Immunology, University of California, Irvine, California 92697, the [§]Department of Biochemistry, College of Medicine, Inje University, Busan 614-735, Korea, [¶]Intellikine, Inc., La Jolla, California 92037, and [‖]Takeda California, Inc., San Diego, California 92121

Background: The class IA PI3K isoform p110α is a promising drug target in cancer therapy yet its role in lymphocytes is not known.
Results: Lymphocyte function was minimally affected by p110α inhibition both *in vitro* and *in vivo*.
Conclusion: Selective inhibition of p110α preserves lymphocyte function.
Significance: The study raises confidence that selective p110α inhibitors in cancer therapy will not be immunosuppressive.

Class IA phosphoinositide 3-kinase (PI3K) is essential for clonal expansion, differentiation, and effector function of B and T lymphocytes. The p110δ catalytic isoform of PI3K is highly expressed in lymphocytes and plays a prominent role in B and T cell responses. Another class IA PI3K catalytic isoform, p110α, is a promising drug target in cancer but little is known about its function in lymphocytes. Here we used highly selective inhibitors to probe the function of p110α in lymphocyte responses *in vitro* and *in vivo*. p110α inhibition partially reduced B cell receptor (BCR)-dependent AKT activation and proliferation, and diminished survival supported by the cytokines BAFF and IL-4. Selective p110δ inhibition suppressed B cell responses much more strongly, yet maximal suppression was achieved by targeting multiple PI3K isoforms. In mouse and human T cells, inhibition of single class IA isoforms had little effect on proliferation, whereas pan-class I inhibition did suppress T cell expansion. In mice, selective p110α inhibition using the investigational agent MLN1117 (previously known as INK1117) did not disrupt the marginal zone B cell compartment and did not block T cell-dependent germinal center formation. In contrast, the selective p110δ inhibitor IC87114 strongly suppressed germinal center formation and reduced marginal zone B cell numbers, similar to a pan-class I inhibitor. These findings show that although acute p110α inhibition partially diminishes AKT activation, selective p110α inhibitors are likely to be less immunosuppressive *in vivo* compared with p110δ or pan-class I inhibitors.

PI3Ks are a family of eight lipid kinase enzymes that produce 3-phosphorylated phosphoinositides in cellular membranes (1). Four of these (p110α, p110β, p110γ, and p110δ) are categorized as class I PI3Ks based on their ability to use phosphatidylinositol 4,5-bisphosphate as a substrate to generate phosphatidylinositol 3,4,5-trisphosphate (PIP_3).[2] The production of PIP_3 leads to recruitment of selected proteins to the membrane and coordinates the assembly of signaling complexes that drive cellular responses to receptor engagement. A hallmark of cancer cells is an elevation in PIP_3, and targeting class I PI3K is a priority in cancer drug discovery (2–5). Each of the class I PI3K catalytic isoforms has been implicated in tumorigenesis and/or maintenance. Of these, p110α has received the most attention because gain-of-function mutations in the *PIK3CA* gene encoding this enzyme are very common in human cancer (6). Mouse models have shown that *PIK3CA* mutations can be drivers of tumorigenesis (7, 8) and cell line studies have shown that the *PIK3CA* mutation status correlates with sensitivity to inhibitors of p110α (9, 10). A distinct PI3K isoform p110β has been suggested to control basal PIP_3 production and drive cancer cells when PTEN, the major PIP_3 phosphatase, is inactivated (11, 12). p110α and p110β are categorized as class IA enzymes because the catalytic subunit forms a dimer with a regulatory subunit containing SH2 domains (p85α, p55α, p50α, p85β, or p55γ). A third class IA catalytic isoform, p110δ, has an emerging role in cancers derived from B lymphoid cells (3). The other class I PI3K catalytic isoform, p110γ, is categorized as class IB because it associates with distinct regulatory subunits (p101 or p84).

It is now appreciated that tumor growth and survival can be either restrained or promoted by cells of the immune system (4, 14, 15). Consequently, it is important to understand how novel anti-cancer drugs impact immune cells. The ideal targeted therapy would enhance anti-tumor immunity while preserving patient immunity to infection. Two class I PI3K isoforms that are highly expressed in leukocytes, p110γ and p110δ, are known

* This work was supported by a sponsored research agreement from Intellikine, Inc. (to D. A. F.).
[1] To whom correspondence should be addressed: 3242 McGaugh Hall, Irvine, CA 92697-3900. Tel.: 949-824-1947; Fax: 949-824-8551; E-mail: dfruman@uci.edu.

[2] The abbreviations used are: PIP3, phosphatidylinositol 3,4,5-trisphosphate; PE, phycoerythrin; APC, Allophycocyanin; CFSE, succinimidyl ester 5-(and -6) carboxyfluorescein diacetate; MZ, marginal zone; pAKT, phosphorylated AKT; TCR, T cell receptor; MTS, 3-(4,5-dimethylthiazol-2-yl)-5-(3-carboxymethoxyphenyl)-2-(4-sulfophenyl)-2*H*-tetrazolium; PHA, phytohemagglutinin; BCR, B cell receptor; GC, germinal center.

to have pleiotropic functions in a variety of immune cells (1, 16). For years there have been useful reagents to study p110γ and p110δ, including selective small molecule inhibitors and mouse strains with null mutations, conditional alleles, and kinase-inactive knock-in alleles. By contrast, little is known about p110α function in the immune system even though this isoform is expressed ubiquitously. Mice with null or kinase-inactive alleles of *Pik3ca* die during embryonic development (17–19). B cell-specific deletion of *Pik3ca* did not reveal a unique function of p110α, but suggested a redundant function with p110δ in peripheral B cell survival (20). p110α deletion in B cells was accompanied by increased p110β expression, potentially compensating for p110α loss (20). Identifying the acute effects of p110α inhibition has been hindered by the absence of highly selective small molecule inhibitors.

In this study, we made use of rationally designed compounds with high selectivity for p110α relative to other PI3Ks and to other cellular kinases. We compared two investigational agents, A66 and MLN1117, along with a set of inhibitors targeting p110β, p110α/p110β, p110δ, or all class I isoforms. The results provide the first evidence that p110α has a measurable quantitative input to AKT phosphorylation and B cell proliferation following BCR cross-linking. However, selective p110α inhibition has a minimal effect overall on B cell and CD4 T cell function, especially when compared with p110δ inhibition. These findings support the hypothesis that p110α inhibitors in clinical trials will not strongly suppress adaptive immune function.

EXPERIMENTAL PROCEDURES

Antibodies—For phospho-flow staining, rabbit antibodies specific for phosphorylated proteins were from Cell Signaling Technologies: Akt (# 4060) and rS6 (# 5364). For flow cytometry and immunohistochemistry, anti-mouse antibodies were: CD4-PE, B220-PE, IgD-eFluor405, IgM-FITC, CD21-FITC, CD23-PE, CD24-PE, CD11d-APC, MOMA-FITC, GL7-Alexa Fluor 647, hCD3-APC, hCD19-PE, DyLight604-conjugated goat anti-rabbit antibody, and streptavidin-conjugated PE or APC (SA-PE/SA-APC). All flow cytometry antibody reagents were purchased from eBioscience and Biolegend. Succinimidyl ester 5-(and -6) carboxyfluorescein diacetate (CFSE), 7-aminoactinomycin D, Fluo-3, and Fura Red were obtained from Invitrogen.

Intracellular Phosphostaining—Intracellular phosphorylation of Akt (S473) and S6 (S240/44) was performed as previously described (21). Briefly, single-cell suspensions of murine splenocytes from 8–12-week-old Balb/c mice were first treated with ACK lysis buffer to remove RBCs. A total of 10^6 cells were treated with different inhibitors for 15 min prior to stimulation using 10 μg/ml of anti-IgM $F(ab')_2$ (Jackson ImmunoResearch) for 15 min in a 37 °C water bath. Cells were immediately fixed with 16% paraformaldehyde stock solutions for a final 1.6% concentration for 10 min at RT. Cells were subsequently washed, then permeabilized with ice-cold methanol for 20 min on ice. Before staining, cells were washed twice in FACS buffer (PBS containing 0.5% BSA and 0.02% sodium azide). Unconjugated primary antibodies were added (pAkt (S473) 1:50, pS6 (S240/44) 1:200) for 1 h at RT. Samples were washed once with FACS buffer and an antibody mixture containing DyLight604-conjugated goat anti-rabbit antibody (1:300) and B220-PE antibody (1:200) was added for 30 min on ice. Specifically for pAkt (S473) analysis, the signal was amplified by using a biotin-conjugated donkey anti-rabbit antibody (1:300; Southern Biotech) for 30 min at RT before adding B220-PE and SA-APC. After staining, cells were washed once with FACS buffer and analyzed on a FACS Calibur equipped with 488- and 635-nm laser lines.

In Vitro Cell Proliferation—SK-OV-3 and U87MG cell lines were obtained from ATCC. A total of 5000 cells/well in low serum media (0.2% FBS) were seeded in triplicate wells of a 96-well flat bottom culture plate for 18 h to adhere. Media was aspirated and inhibitors in 0.2% FBS media were added to each well at the indicated concentrations. After 48 h, cell viability was determined using the MTS assay (Cell Titer 96 Aqueous One solution cell proliferation assay kit; Promega) with absorbance (490 nm) measured in a microplate spectrophotometer.

B Cell Culture—B cells were purified by negative selection using the B cell isolation kit (Miltenyi). For CFSE proliferation assays, purified B cells were labeled with 5 μM CFSE in PBS containing 2% FBS for 5 min at RT. CFSE-labeled B cells were cultured for 3 days in the presence of the indicated inhibitors at a density of 10^6 cells/ml either in 24- or 48-well plates in lymphocyte media (LCM; RPMI medium supplemented with 10% FBS, 100 units/ml of penicillin-streptomycin, 2 mM L-glutamine, 5 mM HEPES buffer, and 50 mM 2-mercaptoethanol). For activation, 10 μg/ml of anti-mouse IgM $F(ab')_2$ (Jackson) with/without IL-4 (10 ng/ml) (R&D Systems) or 10 μg/ml of LPS (Sigma) was used. For survival assays, purified B cells were cultured with either IL-4 (20 ng/ml) or BAFF (60 ng/ml) (Peprotech) for 2 days in culture. Cells were harvested and stained for 7-aminoactinomycin D to analyze cell death by flow cytometry. For human B cells, peripheral blood mononuclear cells were isolated using Ficoll separation from whole blood obtained from the Institute for Clinical and Translational Science at the University of California, Irvine. Peripheral blood mononuclear cells were labeled with CFSE as described above and were activated with anti-IgD dextran (400 ng/ml) and human IL-4 (20 ng/ml) (R&D Systems). After 3 days, cells were harvested and stained with human CD19-PE antibody to gate on B cells.

T Cell Culture—RBC lysed total splenocytes from DO11.10 TCR transgenic mice were labeled with CFSE at a final concentration of 5 μM as described above. After 15 min pre-treatment with the indicated inhibitors, cells were subsequently activated using 10 nM OVA peptide 323–339 (Anaspec) for 3 days in lymphocyte media. After 24 h, 100 μl of supernatants from each sample were collected for cytokine ELISAs. After 3 days, cells were harvested and stained with a CD4-PE antibody to gate on TCR transgenic CD4 T cells. For human T cells, peripheral blood mononuclear cells were isolated from whole blood obtained from the Institute for Clinical and Translational Science, University of California, Irvine. Monocytes and lymphocytes were then purified using a countercurrent elutriation method. On average, 80–90% of the cells were human CD3+ based on flow cytometry. Cells were labeled with CFSE as described above and activated with 1 μg/ml of PHA (Sigma) for 3 days in lymphocyte media. After 3 days, cells were harvested and stained with human CD3-APC antibody to gate on total T cells.

Cytokine ELISA—Supernatants from 24-h activated DO11.10 CD4 T cells were used to detect both mouse IL-2 and IFNγ levels using the Ready-Set-Go ELISA kit (eBioscience). Supernatants from 24-h PHA activated human T cells were used to detect human IL-2 using the Ready-Set-Go ELISA kit (eBioscience) and human IFNg (gamma) using an ELISA kit from BioLegend.

Calcium Flux Assay—Splenocytes were stained with CD1d-biotin, SA-APC, and CD24-PE antibodies prior to loading with the calcium indicator dyes Fluo-3 and Fura Red as described previously (22). Cells were pretreated with the indicated inhibitors for 15 min at 37 °C. The baseline level of Fluo-3/Fura Red was collected for 1 min on a FACS Calibur before cells were stimulated with 10 μg/ml of anti-IgM for 7 min. Cells were then stimulated with 50 ng/ml of ionomycin and acquired for an additional 1 min as a positive control.

In Vivo Dosing of PI3K Inhibitors—Wild-type 8-week-old Balb/cJ mice (Jackson Labs) were used for all experiments. MLN1117 and GDC-0941 were given by oral gavage using a sterile disposable 20-guage 1.5′ feeding needle (Fisher). IC87114 was delivered via intraperitoneal injection. For the non-immunization experiment, 2 mice per group (Vehicle, GDC-0941, and MLN1117) were given the indicated drugs for 9 days before sacrificing on day 10. For the immunization experiment, 4 mice per group were used to perform two independent studies comparing GDC-0941 or IC87114 to MLN1117 as described in the text. In all cases, the vehicle group received both vehicles used to formulate the two different drugs. Mice were treated with the drugs throughout day −1 to day 13. On day 0, all mice were immunized with NP-OVA precipitated in alum (Imject; Pierce). Drug treatment was stopped on day 13 and mice were sacrificed for collection of serum and spleens. Spleens were immediately made into single-cell suspensions for flow cytometric analysis and the rest were quickly frozen in an OCT compound (VWR) for sectioning. For TI-2 immuniza-

TABLE 1

IC_{50} values for inhibition of class I PI3K isoforms and mammalian target of rapamycin (mTOR)

	IC_{50}					
	PI3K class I					
Compound	p110α	p110β	p110γ	p110δ	mTOR	Refs.
	nM				nM	
A66	32	>12,500	3,450	>1,250	>5000	9
MLN1117	15	4,500	1,900	13,900	1,670	
TGX-221	5,000	5	>10,000	100	ND[a]	26
MLN1316	10	8	780	2,200	2,100	
IC87114	>10,000	1,820	1,240	70	ND	27
GDC-0941	3	33	75	3	580	28
ZSTK474	16	44	49	4.6	>10,000	29

[a] ND, not determined.

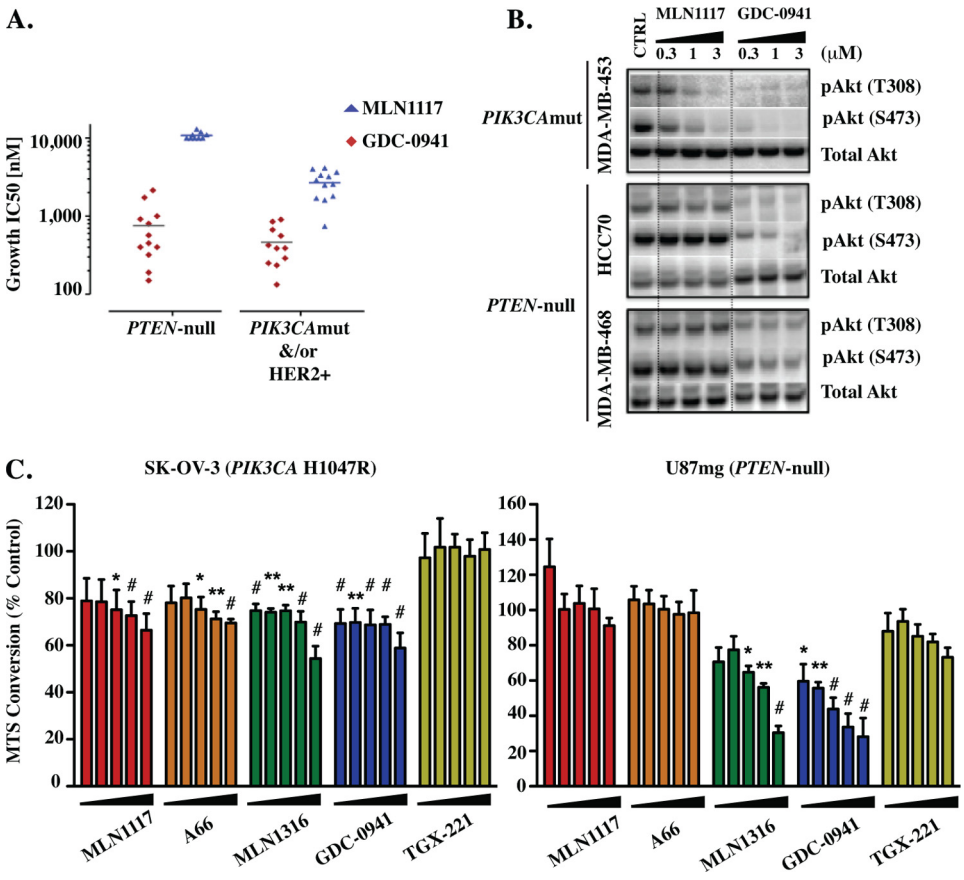

FIGURE 1. **Validation of novel PI3K class IA isoform-selective inhibitors.** *A*, growth IC_{50} values for MLN1117 and GDC-0941 in a panel of breast cancer cell lines harboring a PTEN-null mutation, compared with lines with either a p110α mutation or HER2 overexpression. *B*, phosphorylation status of Akt in response to either MLN1117 or GDC-0941 in three different cell lines harboring the mutations described above. *C*, cell lines (5000 cells/well) either harboring a constitutively activating p110α H1047R mutation (SK-OV-3) or PTEN deletion (U87MG) were cultured under low serum (0.2% FBS) conditions for 48 h in the presence of the indicated inhibitors (2-fold dilution series from right to left: 2, 1, 0.5, 0.25, and 0.125 μM). MTS conversion assay was used to measure viable cell numbers relative to vehicle-treated control (100%) (background-subtracted). Data represent mean ± S.E. of $n = 3$ to 5 experiments (*, $p < 0.05$; **, $p < 0.01$; #, $p < 0.001$, repeated-measures analysis of variance, measured *versus* the vehicle-treated control).

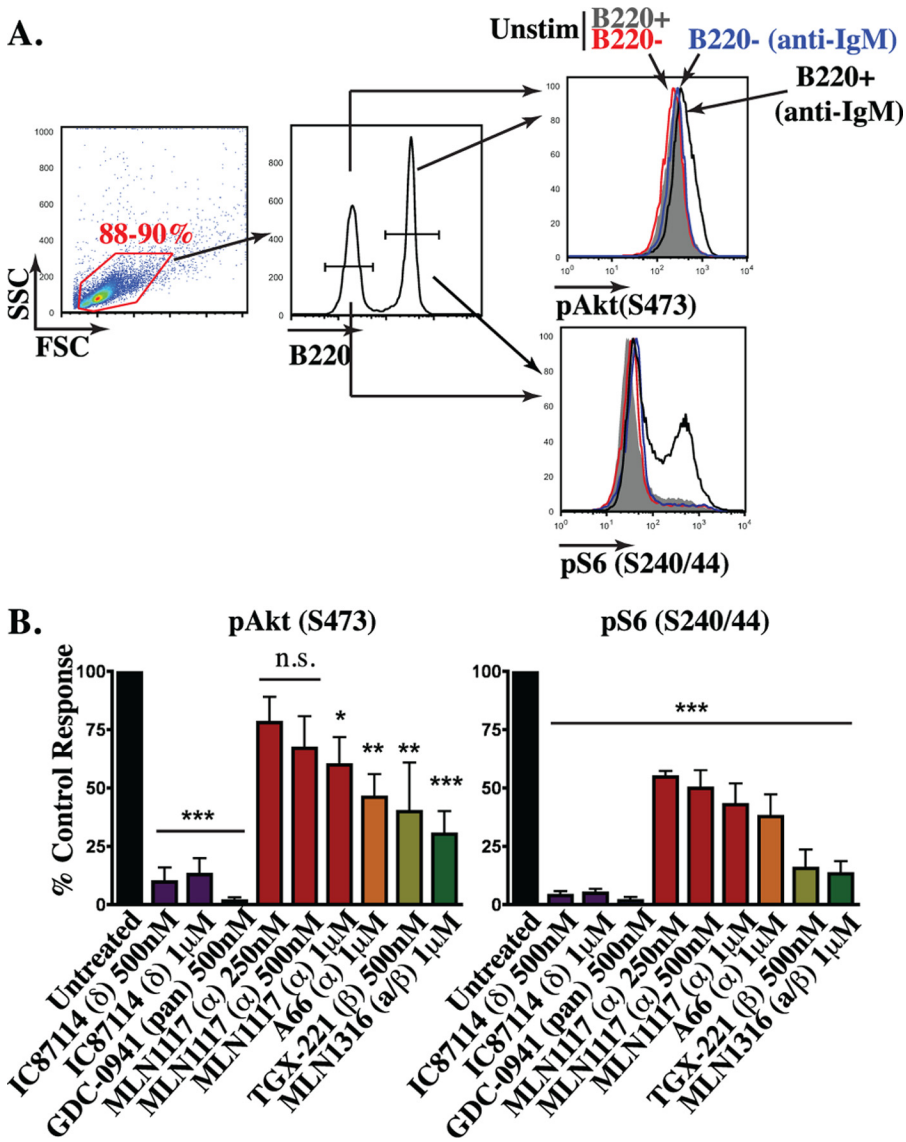

FIGURE 2. **Both p110α and p110β contribute to BCR-mediated PI3K activation in B cells.** *A*, whole splenocytes were incubated with the indicated inhibitors for 15 min and stimulated with 10 μg/ml of anti-IgM for 15 min. Intracellular phosphorylation of pAkt(S473) and pS6(S240/244) were measured at a single cell level by flow cytometry. B cells were distinguished by B220. Selective phosphorylation of Akt and S6 is only observed in the $B220^+$ population (*black*). *B*, data between experiments were normalized by setting the control response as the difference in median fluorescence intensity between the stimulated sample treated with vehicle and the stimulated sample treated with GDC-0941. The % control was averaged from multiple but varying number of experiments for each condition (except pAkt with MLN1117 250 nM ($n = 2$), all conditions were repeated at least three times up to seven times) (*, $p < 0.05$; **, $p < 0.005$; ***, $p < 0.001$, repeated-measures analysis of variance, measured *versus* the vehicle control).

tion, mice were immunized with TNP-Ficoll and serum was collected on day 7.

Serum ELISA—96-Well NUNC MaxiSorp plates (Nalgene) were coated with 50 μl of either NP(30)BSA or NP(3)BSA (Biosearch Technologies) at 50 μg/ml overnight at 4 °C. Serum Ig was detected with HRP-conjugated rabbit anti-mouse secondary antibodies against IgM and IgG1 (Invitrogen). Plates were developed with TMB peroxidase (eBioscience) for colorimetric detection after which the reaction was stopped with 1 N sulfuric acid and read on a plate reader at 450 nm. For TNP-Ficoll immunization, plates were coated with 100 μl of TNP-BSA at a concentration of 10 μg/ml for 1½ h at room temperature. Serum Ig was detected with HRP-conjugated goat anti-mouse secondary antibodies against IgG3 (Southern Biotech). Plates were developed as described above.

Immunohistochemistry—Mouse spleens embedded in OCT medium were frozen and 8-μm sections were cut and mounted on Superfrost Plus slides (Fisher Scientific). Slides were fixed in acetone at −20 °C for 20 min and blocked with FACS buffer for 30 min at room temperature. Immunohistochemical staining was done with anti-mouse antibodies against IgD-eFluor405, IgM-FITC, and GL7-Alexa Fluor647 (all 1:100 dilution) for 1 h at room temperature, followed by three 5-min washes in PBS. Marginal zone (MZ) B cells were identified as IgM-bright, IgD-dim cells surrounding IgM-dim, IgD-bright follicles. Germinal center B cells were identified as IgD-negative, GL7-positive. For some sections, antibodies against B220-PE and metallophilic macrophage (MOMA-1)-FITC were used as an alternative method to identify MZ B cells (B220-positive cells outside the MOMA-1 border). All images shown were acquired at either

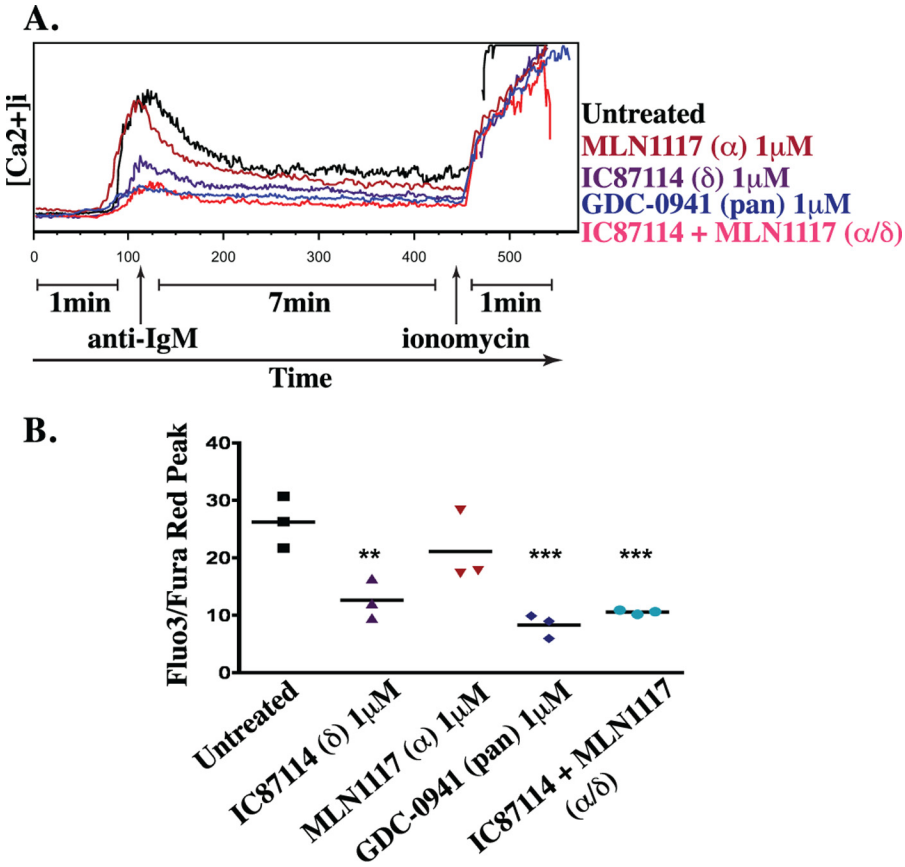

FIGURE 3. **BCR-mediated Ca^{2+} mobilization is mainly p110δ-dependent.** *A*, kinetics of calcium mobilization was monitored using ratiometric measurement of Fluo-3 and Fura Red fluorescence. FO B cell population was distinguished by flow cytometry (CD24 and CD1d). Data are representative of three independent experiments. *B*, the peak Ca^{2+} response after anti-IgM-mediated BCR cross-linking was plotted for three independent experiments (**, $p < 0.005$; ***, $p < 0.001$, repeated-measures analysis of variance, measured *versus* the untreated control).

×10 or 20 magnification using Olympus Fluoview FV1000 Laser Scanning Confocal Microscope.

RESULTS

PI3K Inhibitor Validation—The inhibitors used in this study are listed in Table 1 along with their isoform selectivity defined by *in vitro* kinase activity assays using recombinant enzymes. We used two p110α-selective inhibitors with distinct chemical structure, to minimize possible off-target effects. A66 has been studied previously in preclinical cancer models (9, 23). MLN1117, originally described by Intellikine as INK1117 (24), is currently in phase I trials for patients with advanced solid tumors (clinical trials identifier NCT01449370). To inhibit p110β we used TGX-221 (25, 26). This compound has some activity against p110δ (IC_{50} 100 *versus* 5 nM for p110β; Table 1). As another means to inhibit p110β, we used the compound MLN1316, a dual p110α/p110β inhibitor that is highly selective relative to p110δ and p110γ (Table 1). We used IC87114 as a p110δ inhibitor (27–29). To inhibit all class I isoforms, we used the two compounds GDC-0941 (11, 30, 31) and ZSTK474 (32, 33). *In vitro*, both compounds inhibit all class I isoforms with IC_{50} values between 3 and 75 nM with some preference for p110α and p110δ (Table 1). ZSTK474 is more selective than GDC-0941 with respect to mammalian target of rapamycin (Table 1). The selectivity of MLN1117 compared with GDC-0941 is supported by studies of breast cancer cell lines (Fig. 1, *A* and *B*). MLN1117 inhibits AKT phosphorylation and growth in *PIK3CA* mutant breast cancer cells with IC_{50} values around 2 μM, yet has no effect on cells lacking *PTEN*. In contrast, GDC-0941 has similar effects on cell lines with *PI3KCA* mutation or *PTEN* loss.

We further validated the selectivity of the inhibitor panel using cancer cell lines previously shown to be driven primarily by p110α or p110β. SK-OV-3 (*KRAS* wild-type) has an activating *PIK3CA* mutation and was shown previously to be sensitive to A66 (9). The cancer cell line U87MG lacks PTEN and is preferentially sensitive to p110β inhibition (34). Cells were cultured for 2 days with titrated amounts of inhibitors before measurement of viable cell number by M3-(4,5-dimethylthiazol-2-yl)-5-(3-carboxymethoxyphenyl)-2-(4-sulfophenyl)-2*H*-tetrazolium assay (MTS) (Fig. 1*C*). Low serum conditions were used to increase cell dependence on endogenous PI3K activation. As expected, A66 and MLN1117 reduced growth of SK-OV-3 over a concentration range from 125 nM to 2 μM. Statistically significant effects were seen from 500 nM to 2 μM. In U87MG cells, A66 and MLN1117 had no effect at these concentrations. MLN1316 at concentrations of 500 nM to 2 μM reduced viable cell number of both SK-OV-3 and U87MG cells. Together these data show that 1 μM concentrations of each inhibitor selectively inhibit growth and/or survival of cancer cells driven by the appropriate target, p110α or p110β. Previous

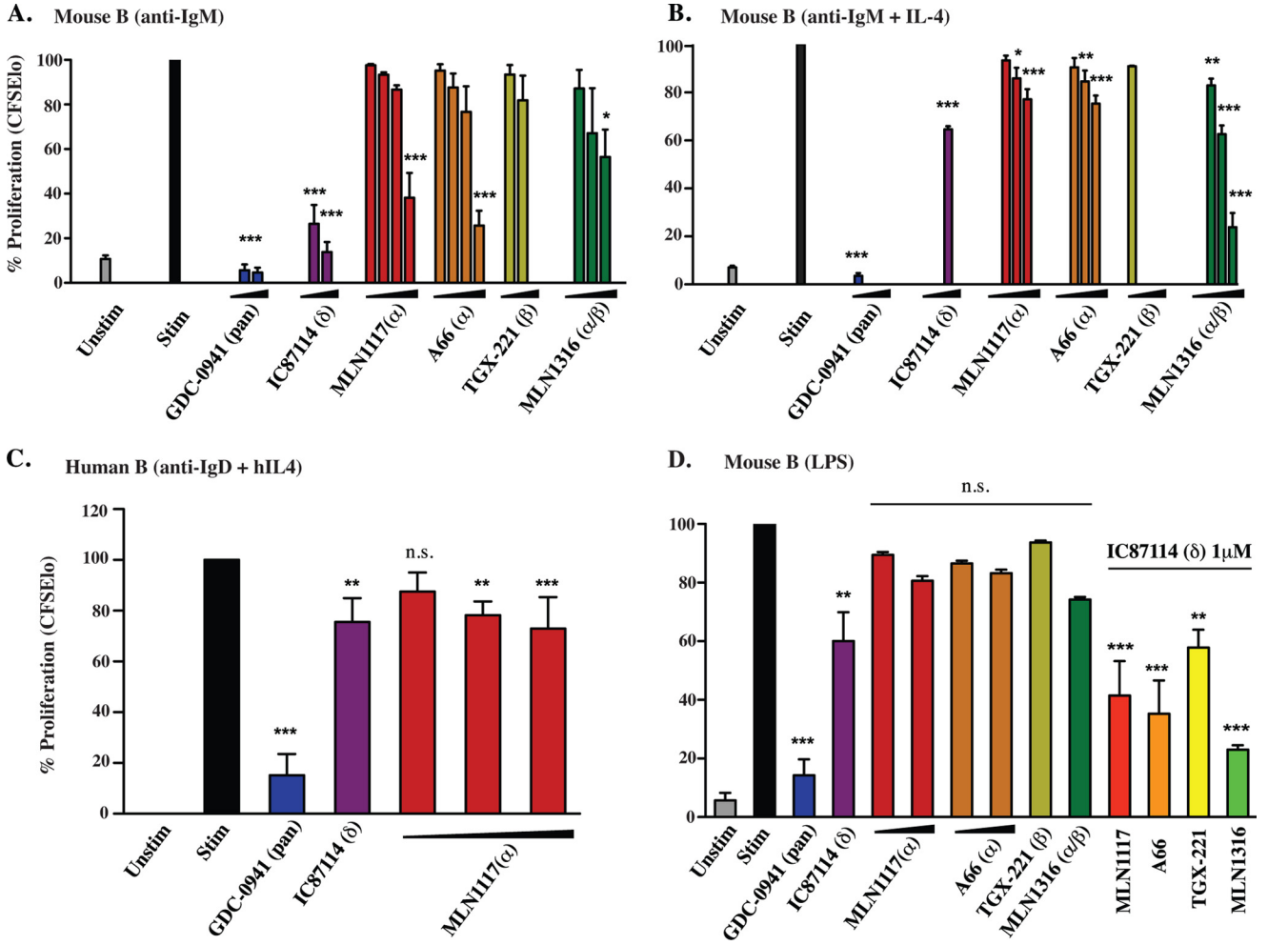

FIGURE 4. **p110δ is the primary PI3K isoform that contributes to B cell proliferation.** *A*, anti-IgM-mediated B cell proliferation from three independent experiments was normalized to a percentage scale. Concentrations used were MLN1117 and A66 (0.25, 0.5, 1, and 2 μM), TGX-221 (0.25, 0.5 μM), MLN1316 (0.25, 0.5, and 1 μM), GDC-0941 (0.25 and 0.5 μM), and IC87114 (0.5 and 1 μM). *B*, anti-IgM + IL4-mediated B cell proliferation from three independent experiments was normalized to a percentage scale. Concentrations used were MLN1117, A66, and MLN1316 (0.5, 1, and 2 μM), TGX-221 (0.5 μM), GDC-0941 (0.5 μM), and IC87114 (1 μM). *C*, anti-IgD + IL-4-mediated human B cell proliferation from three independent experiments was normalized to a percentage scale. Concentrations used were MLN1117 (0.5, 1, and 2 μM), GDC-0941 (0.5 μM), and IC87114 (1 μM). *D*, three independent experiments of LPS-mediated B cell proliferation were analyzed in a similar manner to *B*. 1 μM concentration was used for all inhibitors except GDC-0941 (0.5 μM) and TGX-221 (0.5 μM). In the combination treatments, IC87114 (1 μM) with 1 μM of the indicated inhibitors was used. All data represent results from at least three independent experiments (*, $p < 0.05$; **, $p < 0.005$; ***, $p < 0.001$, repeated-measures analysis of variance, measured *versus* the untreated control).

studies have shown that IC87114 is specific for p110δ when cells are treated with 1 μM of this compound (29). TGX-221 did not cause a significant effect in these experiments but showed a trend toward inhibiting the cell number of U87MG at 500 nM to 2 μM. Based on these considerations we used a maximum concentration of 0.5–1 μM of each inhibitor for most experiments.

B Cell Signaling—Genetic or pharmacological inactivation of p110δ strongly blocks BCR-mediated AKT activation and proliferation (16, 35). These observations support the model that p110δ is the primary PI3K catalytic isoform engaged by BCR signalosomes. We confirmed that IC87114 blocks pAKT induction nearly to the same extent as the pan-class I inhibitor, GDC-0941 (Fig. 2). However, BCR-stimulated B cells treated with 1 μM A66 or MLN1117 displayed a significant reduction (up to 50%) in the magnitude of the phosphorylated AKT (pAKT) signal measured by intracellular flow cytometry (Fig. 2). The effect of MLN1117 was dose-dependent. The p110β inhibitor TGX221 and the dual p110α/β inhibitor MLN1316 also significantly reduced the pAKT detected. We assessed AKT activity indirectly by measuring BCR-mediated phosphorylation of ribosomal protein S6 (pS6), a readout of S6 kinase activity downstream of PI3K/AKT/mTORC1 (22). Again we observed that inhibitors of p110α and/or p110β partially reduced pS6, whereas IC87114 strongly suppressed pS6 to a degree similar as GDC-0941. A plausible interpretation of these data is that p110δ, p110α, and p110β each contribute to PIP_3 production by BCR cross-linking, but that p110δ inhibition reduces PIP_3 below a threshold required to sustain AKT activation.

A major function of class IA PI3K in BCR signaling is to promote activation of PLCγ to drive Ca^{2+} mobilization (16, 36). As reported previously (27), IC87114 significantly suppressed the Ca^{2+} response of B cells stimulated with anti-IgM (Fig. 3). The effect of IC87114 appeared less complete than GDC-0941, but the difference in peak intracellular Ca^{2+} was not significant. The Ca^{2+} peak in cells treated with MLN1117 did not show a statistically significant difference compared with diluent con-

trol. These observations confirm that p110δ is the dominant isoform linking BCR engagement to Ca^{2+} mobilization.

B Cell Proliferation and Survival—We compared the effects of inhibitors on the proliferation of purified, CFSE-labeled B cells. In cells stimulated through the BCR with anti-IgM, p110δ inhibition blocked cell division nearly to the same extent as pan-class I PI3K inhibition. Fig. 4*A* shows a graph of the average proliferation over multiple experiments, expressed as the percent of divided (CFSE-low) cells. Statistical analysis of normalized data showed that the effects of GDC-0941 and IC87114 were highly significant, yet there was no significant effect of 1 μM A66, MLN1117, or TGX-221. At a higher concentration (2 μM), A66 or MLN1117 did significantly suppress B cell proliferation driven by anti-IgM alone but not by anti-IgM plus IL-4 (Fig. 4, *A* and *B*). Notably, CFSE histograms for three independent experiments did show a consistent, dose-dependent reduction in the extent of B cell division by each of the isoform-selective PI3K inhibitors (data not shown). We obtained similar results using human peripheral blood B cells stimulated with anti-human IgD and IL-4 (Fig. 4*C*).

GDC-0941 caused a marked increase in B cell death, as suggested by the reduced cell recovery (data not shown) and confirmed by measuring the percentage of cells staining with DAPI nuclear dye (anti-IgM; untreated: *versus* GDC-0941 0.5 μM: 38 *versus* 95%). IC87114 had an intermediate effect on B cell death (75%) and there was only a minor effect of p110α inhibitors at the selective concentration of 1 μM.

The bacterial cell wall component lipopolysaccharide (LPS) causes polyclonal B cell proliferation through a TLR4-dependent pathway. In LPS-stimulated mouse B cells, IC87114 was the only isoform-selective inhibitor to significantly reduce the percent of divided cells (Fig. 4*D*). However, under these conditions IC87114 did not block proliferation to the same degree as GDC-0941 nor did IC87114 cause death of LPS-stimulated cells (GDC-0941 *versus* IC87114: 77 versus 33%). Examination of the CFSE dilution data suggested that MLN1316 measurably reduced cell division, and combining IC87114 with MLN1316 blocked cell division more fully (data not shown). These data suggest that each class IA isoform contributes to LPS-driven B cell proliferation. However, selective p110α inhibition had a negligible effect.

Next we tested the effects of PI3K inhibitors on survival of purified B cells cultured in the presence of the cytokines BAFF or IL-4. Both GDC-0941 and IC87114 blocked cytokine-dependent survival even at the low concentration of 250 nM, and GDC-0941 reduced viability below the level observed in cells cultured without cytokines or inhibitors (Fig. 5). In contrast, even at higher concentrations (1 μM) both A66 and MLN1117 caused only a minor decrease in survival. When p110α inhibitors were combined with IC87114 there was a trend toward additive suppression of survival, but this was not statistically significant. TGX-221 partially reduced B cell survival, and the dual p110α/β inhibitor MLN1316 appeared to have a greater effect especially in BAFF-treated cells.

In summary, our studies of B cells *in vitro* indicate that acute p110α inhibition measurably reduces BCR-mediated AKT phosphorylation but causes only incremental decreases in Ca^{2+} flux, proliferation, and survival. Likewise, the B cell response to

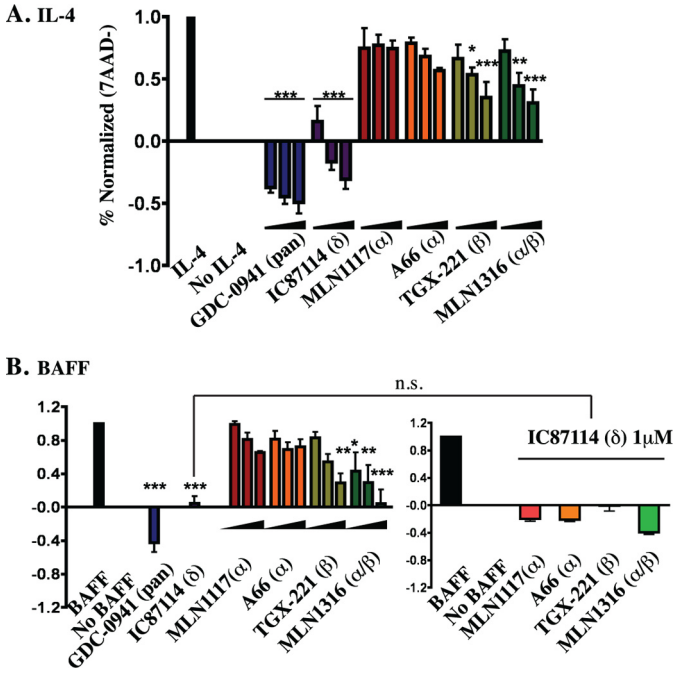

FIGURE 5. **Inhibition of p110α does not significantly reduce IL-4 or BAFF-mediated B cell survival.** Purified B cells were cultured in B cell media containing either IL-4 (*A*) or BAFF (*B*) for 48 h and cell viability was measured using 7-aminoactinomycin D exclusion. Viable cells (%7-aminoactinomycin D negative) were normalized for three independent experiments. For each indicated inhibitor, the three concentrations used were 0.25, 0.5, and 1 μM. *B,* for BAFF survival experiments, single concentrations of GDC-0941 (0.5 μM) and IC87114 (1 μM) were used. In the combination treatments (*bottom right*), IC87114 (1 μM) with 1 μM of the indicated inhibitors were used. Normalized data of the combination treatments are from the same experiments of single treatments (*bottom left*). All data represent results from at least three independent experiments (*, $p < 0.05$; **, $p < 0.005$; ***, $p < 0.001$, repeated-measures analysis of variance, measured *versus* the untreated control).

LPS and survival cytokines is mediated predominantly through p110δ with lesser contributions of p110α and p110β.

T Cell Proliferation—Initial studies of p110δ-deficient mice showed a profound block of BCR-mediated proliferation, whereas T cells from these mice proliferated relatively normally in response to co-clustering of the T cell receptor (TCR) with the costimulatory molecule CD28 (37). Subsequent experiments using TCR transgenic T cells showed that p110δ plays a more prominent role in clonal expansion of antigen-specific CD4 T cells (38). In addition, the p110δ-selective inhibitor IC87114 was reported to inhibit proliferation of both mouse and human T cells (29). An important caveat is that when present at concentrations above 1 μM, IC87114 inhibits proliferation of T cells with inactive p110δ (29). Therefore, cellular effects of IC87114 above 1 μM might result from achieving a more pan-PI3K inhibition profile. Here we compared the effects of 1 μM IC87114 and other PI3K inhibitors on T cell proliferation. For murine cells, we measured the proliferation of DO11.10 transgenic T cells stimulated with cognate OVA peptide in the presence of autologous splenocytes. For human cells, we used peripheral blood T cells stimulated with the polyclonal activator PHA.

As shown in Fig. 6*A*, the proliferation of DO11.10 T cells in the presence of 10 nM OVA peptide was only marginally reduced by individual inhibitors of class I isoforms. 1 μM A66, MLN1117, TGX-221, or IC87114 did not significantly decrease the percentage of divided cells, but CFSE histogram overlays

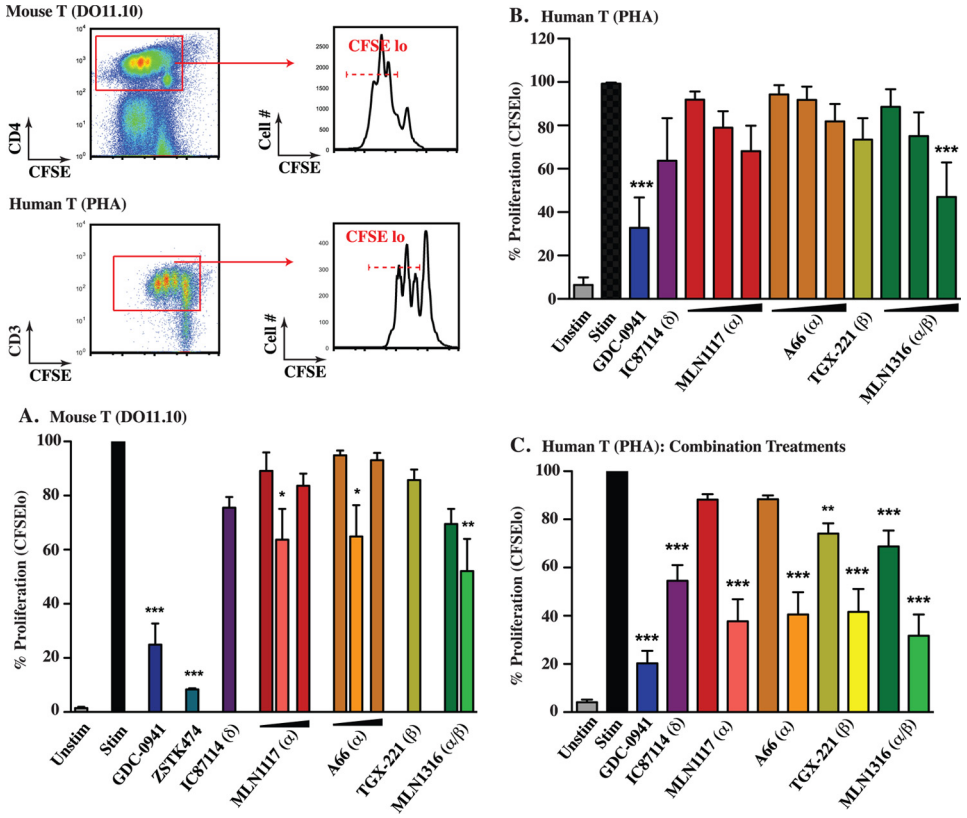

FIGURE 6. **PI3K class IA isoforms have redundant functions in antigen-mediated T cell proliferation.** *A*, CFSE labeled whole splenocytes from DO11.10 TCR transgenic mouse were activated with 10 nM $OVA_{323–329}$ peptide for 3 days. $CD4^+$ T cells were gated and proliferation was normalized to a percentage scale (gating scheme is presented in the *top left* of figure). 1 μM concentration was used for all inhibitors except for MLN1117 and A66 (1 and 2 μM). In the combination treatments (depicted by the *lighter color* next to MLN1117, A66, and MLN1316), IC87114 (1 μM) with 1 μM of the indicated inhibitors was used. *B*, human T cells were activated with 1 μg/ml of PHA for 3 days. $CD3^+$ total T cells were gated and proliferation was normalized to a percentage scale (gating scheme is presented in the *top left* of figure). Concentrations used were MLN1117, A66 and MLN1316 (0.5, 1, nd 2 μM), TGX-221 (1 μM), GDC-0941 (0.5 μM), and IC87114 1 μM. *C*, same experiment as in *B* with combination treatments. 1 μM concentration was used for all inhibitors except for GDC-0941 (0.5 μM) and TGX-221 (0.5 μM). In the combination treatments (depicted by the *lighter color* next to MLN1117, A66, TGX-221, and MLN1316), IC87114 (1 μM) with each indicated inhibitor was used. All data represent results from at least three independent experiments (*, $p < 0.05$; **, $p < 0.005$; ***, $p < 0.001$, repeated-measures analysis of variance, measured *versus* the untreated control).

showed that each inhibitor mildly restrained cell division (data not shown). Increasing the concentration of MLN1117 or A66 to 2 μM did not cause greater inhibition of cell division. Combining IC87114 with A66, MLN1117, or MLN1316 did significantly reduce the proliferative response although the overall percentage of divided cells was diminished less than 50%. The pan-class I inhibitor GDC-0941 significantly blocked proliferation in T cells stimulated with 10 nM OVA, although in most experiments the inhibition was incomplete (Fig. 6*A* and data not shown). The compound ZSTK474 was a more effective inhibitor of antigen-driven T cell proliferation (Fig. 6*A* and data not shown). Whether the greater efficacy of ZSTK474 is attributable to slightly greater inhibition of p110γ (Table 1) or other pharmacological differences is unclear. Together these findings indicate that multiple class I PI3K isoforms contribute to the overall function of PI3K signaling during T cell expansion. Very similar results were obtained using PHA-stimulated human T cells (Fig. 6, *B* and C).

The cytokine interleukin-2 (IL-2) is produced by activated T cells and acts as an autocrine and paracrine growth factor to drive proliferation. Consistent with the cell division data, selective blockade of individual PI3K isoforms partially reduced IL-2 production, whereas the response was inhibited almost completely by drug combinations or by the pan-PI3K inhibitors GDC-0941 and ZSTK474 (Fig. 7, *A* and *B*). T cell secretion of the cytokine interferon-γ (IFNγ) seemed generally more sensitive to PI3K inhibition, with p110α and p110β inhibitors having significant effects in mouse T cells (Fig. 7*C*). Nevertheless, the overall pattern for mouse IFNγ and IL-2 was comparable with IC87114 having stronger effects especially when combined with p110α and p110β inhibitors. Secretion of IFNγ by human T cells stimulated with PHA showed variability among donors but the overall pattern was similar (Fig. 7*D*).

Lymphocyte Function in Vivo—Last we evaluated the effects of different PI3K inhibitors on lymphocyte subsets and function *in vivo*. For treatments with GDC-0941 or MLN1117, we used doses and formulations shown to provide anti-cancer efficacy in solid tumor xenograft models (31).[3] For treatment with IC87114, we used a dose and treatment protocol previously shown to reduce MZ B cell numbers in mice (28). Daily treatment with MLN1117, IC87114, or GDC-0941 did not alter the percentages or numbers of T cells, and did not affect the ratio of CD4 and CD8 T cells relative to vehicle-treated controls (data not shown).

[3] L. V. Kessler, J. M. Kucharski, L.-S. Li, M. B. Martin, P. Ren, K. A. Jessen, Yi Liu, and C. Rommel, unpublished data.

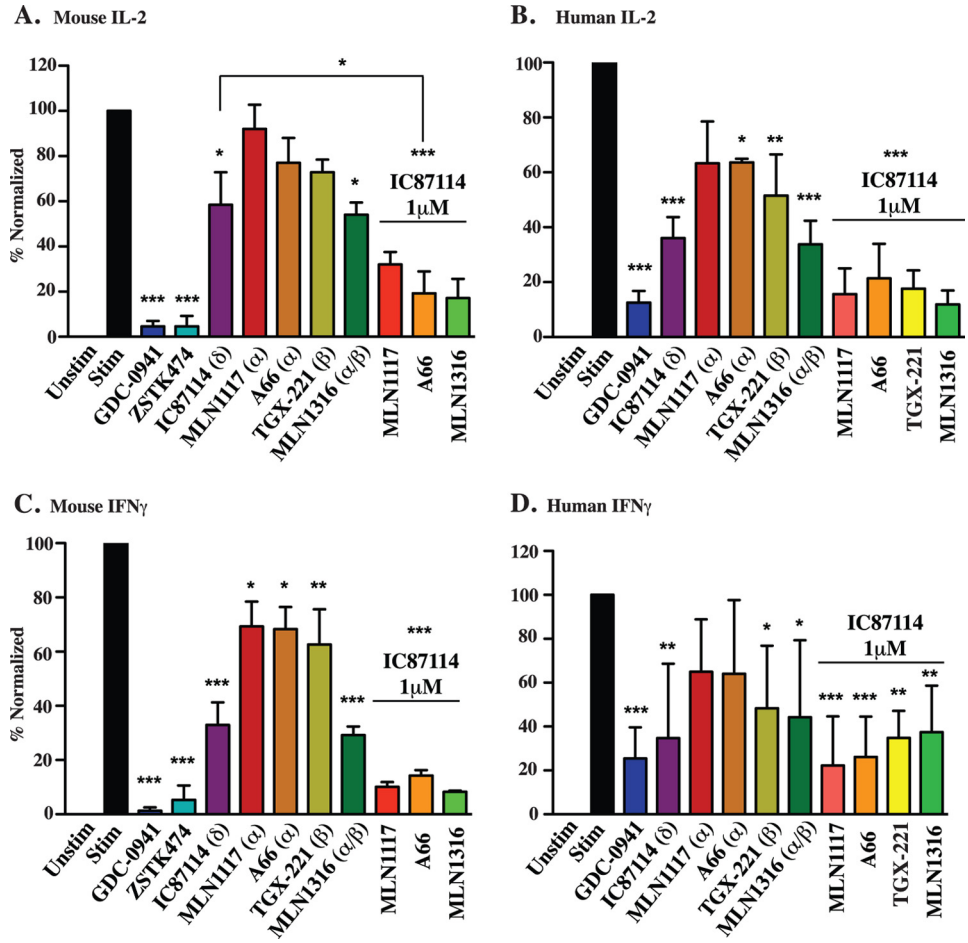

FIGURE 7. **PI3K class IA isoforms have redundant functions in T cell cytokine production.** IL-2 (*A* and *B*) and IFNγ (*C* and *D*) levels were measured by ELISA from the supernatants in Fig. 6 after 24 h activation with $OVA_{323–329}$ peptide or PHA. Cytokine levels were normalized to a percentage scale from three independent experiments. 1 μM concentration for all inhibitors except GDC-0941, ZSTK474, and TGX-221 (0.5 μM) are shown.

Genetic inactivation of p110δ causes a large reduction in the number of MZ B cells, a specialized B cell subset in the mouse spleen that responds mainly to T cell-independent antigens (37). Similarly, pharmacological inhibition of p110δ with IC87114 *in vivo* causes aberrant localization of MZ B cells (28). In accord, we detected fewer MZ B cells ($IgM^{hi}IgD^{lo}$) in spleen sections of mice treated with IC87114 or the pan class I inhibitor GDC-0941 (Fig. 8*A*). Based on FACS-based discrimination of splenic B cell subsets, we also found that IC87114 and GDC-0941 reduced the overall percentage of MZ B cells (Fig. 8*B*; MZ cells are identified as $CD21^{hi}CD23^{lo}$ by FACS). In contrast, mice treated with MLN1117 displayed no change in the percentage or localization of MZ B cells (Fig. 8, *A* and *B*). These results are consistent with a required role for p110δ but not p110α in the MZ B cell compartment. These experiments were carried out in mice immunized with NP-OVA (see below), but similar effects on MZ B cells were observed in non-immunized mice as well (data not shown).

To compare the effects of PI3K inhibitors on B cell and T cell-mediated immune responses *in vivo*, we measured antibody production in mice vaccinated with hapten-carrier conjugates. To model T cell-independent antibody responses driven by BCR cross-linking, we used TNP-Ficoll as the immunogen. GDC-0941 treatment abrogated TNP-specific IgG3 production (Fig. 9*A*). This indicates that the T cell-independent IgG3 response is completely PI3K dependent. Treatment with MLN1117 at 30 and 60 mg/kg caused little reduction of TNP-specific IgG3 (Fig. 9*A*). Notably, we did observe reduction of TNP-specific IgG3 at higher doses of MLN1117 (120 mg/kg), consistent with the partial reduction in cell division in B cells treated with MLN1117 before anti-IgM stimulation *in vitro*. However, 120 mg/kg is above the effective dose of MLN1117 for tumor growth inhibition (30–60 mg/kg).

To model a T cell-dependent antibody response, we used NP-OVA as the immunogen. In this case, treatment with MLN1117 (60 mg/kg) did not diminish the NP-specific IgM or IgG1 responses (Fig. 9*B*). This is consistent with the minimal effect of MLN1117 on T cell proliferation *in vitro* and on B cells stimulated with anti-IgM plus IL-4. To our surprise, mice treated with IC87114 or GDC-0941 also produced normal NP-specific antibody titers and affinity (Fig. 9*B* and data not shown). The absence of drug effects was not likely due to poor pharmacokinetics as both IC87114 and GDC-0941 impacted the MZ B cell compartment at these doses (Fig. 8). Furthermore, as reported previously (39), selective p110δ inhibition with IC87114 augmented the antigen-specific IgE response (Fig. 9*B*, *lower right graph*). Staining of spleen sections revealed that both IC87114 and GDC-0941, but not MLN1117, reduced

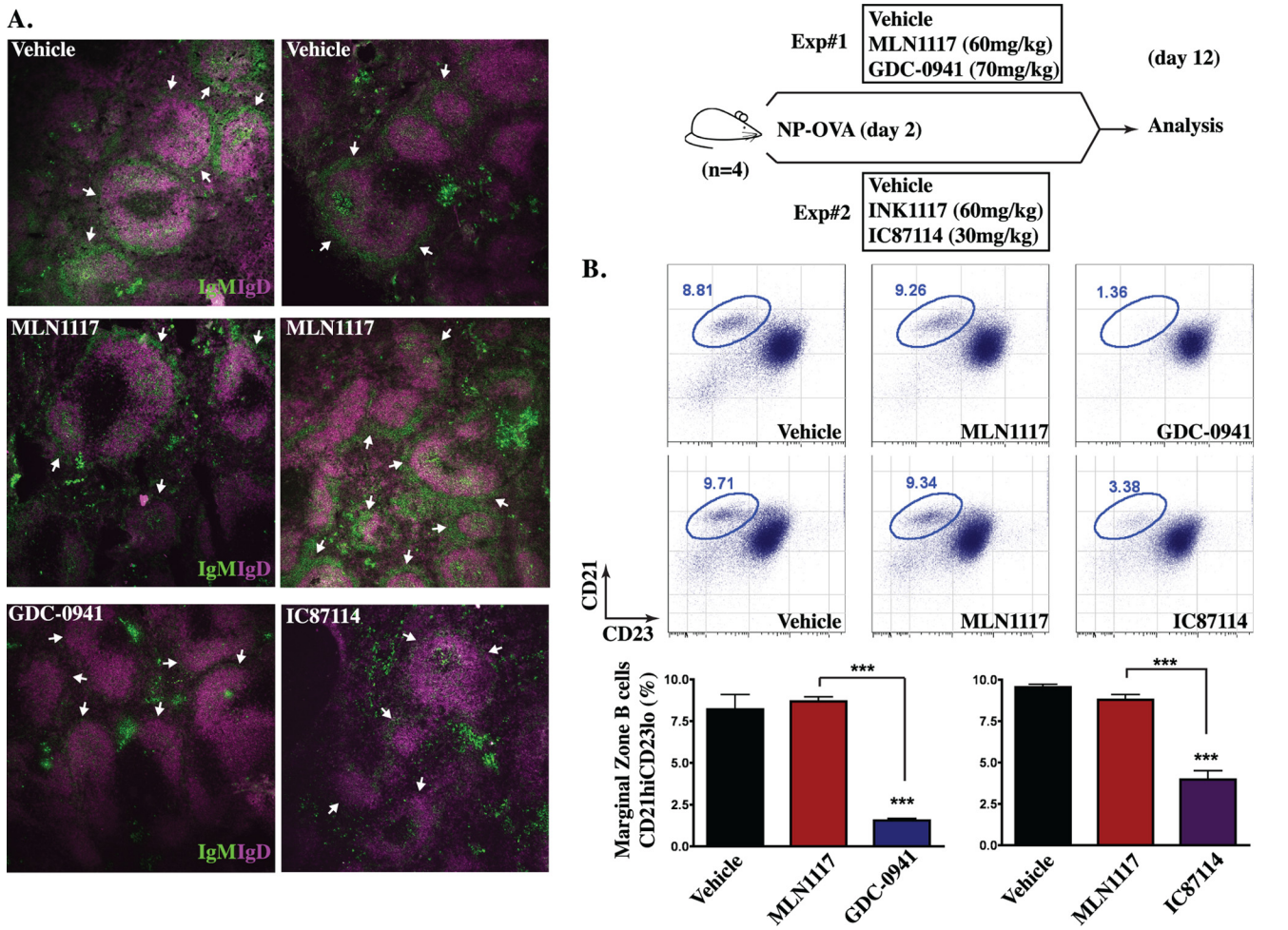

FIGURE 8. **GDC-0941 and IC87114, but not MLN1117, decrease the MZ B cell compartment *in vivo*.** Two independent experiments (*top right*) were conducted where the *in vivo* effects of GDC-0941 and IC87114 compared with MLN1117 were assessed. Mice ($n = 4$ mice per group) were given the drugs daily for 11 days and were immunized on day 2 with a T-dependent antigen NP-OVA. *A,* mouse spleen sections from each treated mouse were stained with anti-IgM-FITC and anti-IgD-eFluor405 to distinguish MZ B cells ($IgM^{hi}IgD^{lo}$) from FO B cells ($IgM^{lo}IgD^{hi}$). All images are representative of multiple spleen sections from different mice ($n = 4$ mice per group). *B,* total splenocytes harvested on day 12 were stained with CD21-FITC and CD23-PE to identify MZ B cells ($CD21^{hi}CD23^{lo}$) by flow cytometry. Flow plots are representative splenocyte staining data from multiple mice (data not shown per group). MZ B cell frequency from four different mice is shown as a bar graph (***, $p < 0.001$, analysis of variance, measured *versus* the vehicle-treated mice, except where indicated by *brackets*). The MZ B cell compartment was also assessed in non-immunized mice treated with MLN1117 or GDC-0941 (data not shown).

the appearance of B cells with a germinal center (GC) phenotype ($IgD^{lo}GL7+$) in NP-OVA-immunized mice (Fig. 9, *C* and *D*). The distinct effects of MLN1117 and GDC-0941 on GC B cell numbers were confirmed by flow cytometry (data not shown). Thus, selective pharmacological inhibition of p110α does not noticeably alter B cell survival, localization, or antibody production *in vivo*.

DISCUSSION

In this study we have used novel PI3K isoform-selective inhibitors to probe the function of p110α in B and T cells. The results show for the first time that this isoform has a measureable contribution to PI3K signaling output and lymphocyte function. Nevertheless, selective inhibition of p110α (and/or p110β) does not strongly impair lymphocyte proliferation or survival *in vitro*. Moreover, treating mice with the p110α inhibitor MLN1117 at doses with anti-tumor activity in preclinical models does not interfere with T cell-dependent antibody responses. In contrast, the pan-class I inhibitor GDC-0941 and the selective p110δ inhibitor IC87114 strongly uppress B cell proliferation and survival *in vitro* and impairs germinal center responses *in vivo*.

Our observation that p110α inhibition reduces BCR-dependent AKT phosphorylation and proliferation contrasts with a study showing normal responses in B cells with conditional deletion of the *Pik3ca* gene encoding p110α (CD2Cre-$p110\alpha^{fl}$) (20). Notably, B cells from CD2Cre-$p110\alpha^{fl}$ mice display marked up-regulation of the p110β isoform (20). Our data indicate that p110β functions in BCR-mediated proliferation and survival. Hence, p110β up-regulation might compensate for loss of p110α, masking the function that is revealed by acute pharmacological inhibition of p110α in mature B cells. Interestingly, the substantial loss of pAKT and pS6 in BCR-stimulated cells pretreated with p110α inhibitors did not correlate with a strong block in proliferation. Rather, these compounds caused only a modest reduction in BCR-mediated cell division that matched more closely with the Ca^{2+} flux response. This fits with the model that the most important function of PI3K in

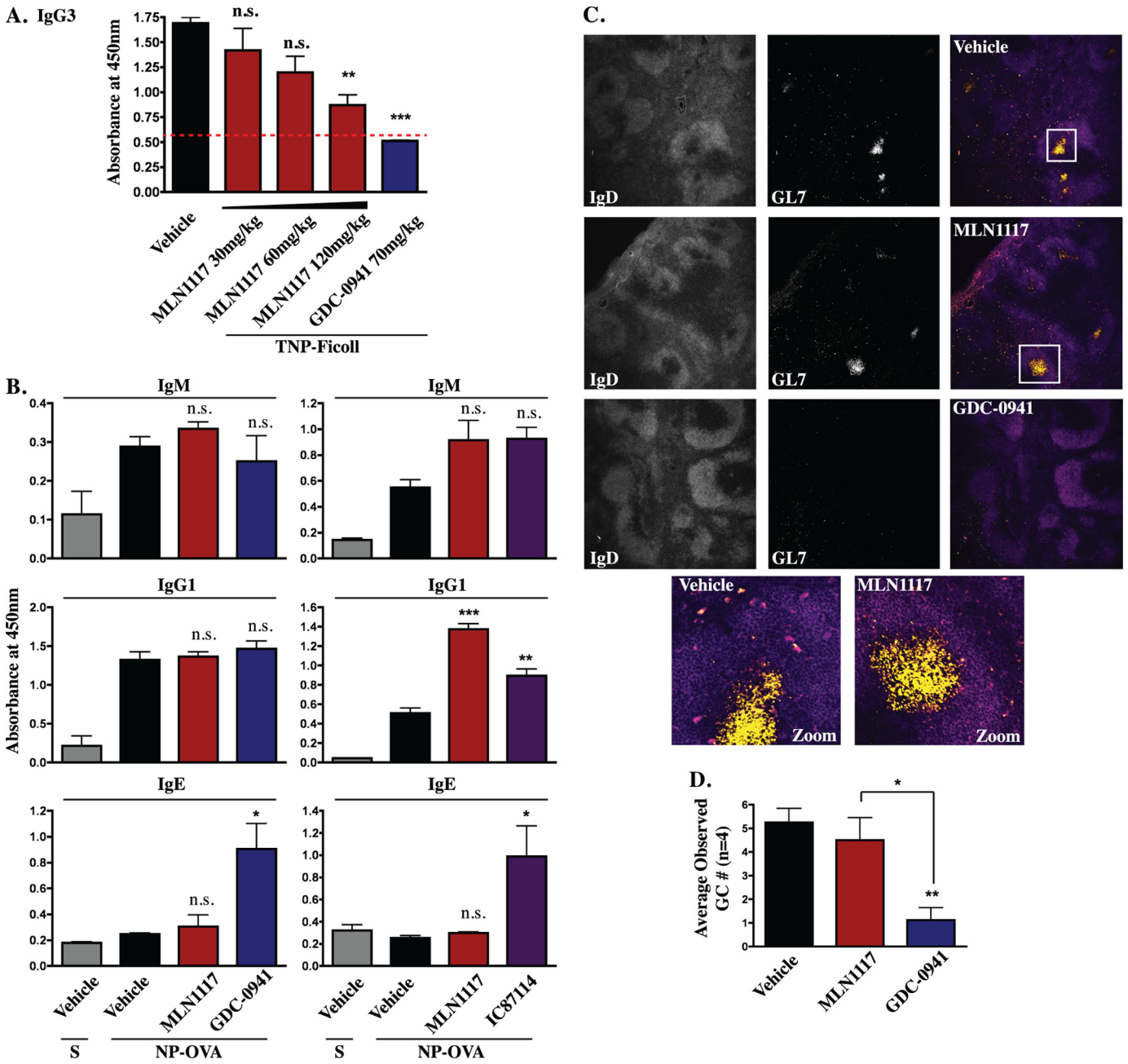

FIGURE 9. **MLN1117 does not diminish the germinal center (*GC*) response or production of NP-specific antibody *in vivo*.** *A*, mice ($n = 6$ per group) were immunized with TNP-Ficoll and given the drugs at the indicated doses for 7 days. Quantification of TNP-specific IgG3 in serum was done by ELISA using TNP-BSA-coated plates (**, $p < 0.01$; ***, $p < 0.001$, analysis of variance, measured *versus* the vehicle-treated mice, except where indicated by *brackets*: *N.S.*, non-significant). The *dotted line* indicates the lower limit of linearity of detection. *B*, mice ($n = 4$) per group were immunized with NP-OVA and treated for 13 days. Quantification of nitrophenyl (*NP*)-specific IgM, IgG1, and IgE in serum by ELISA was done using NP(30)-BSA coated plates. *S*, sham immunized. *C*, spleen sections from each treated mouse were stained with anti-IgD-eFluor405 and anti-GL7-Alexa Fluor647 to distinguish GCs ($IgD^{low}GL7^{+}$) within the follicles. T cell zones were distinguished by a separate CD4-FITC staining (data not shown) and were concentrated outside the follicles. *D*, quantification of GC numbers per mouse. Two random areas from each slide (spleen sections from one mouse on each slide, $n = 4$ mice per group) were observed for GCs ($IgD^{low}GL7^{+}$) and counted by two different lab members in blinded fashion (slide labels were hidden). The total GC counts per treatment group were divided by the number of mice ($n = 4$) to achieve the observed GC numbers per mouse for each treatment (*, $p < 0.05$; **, $p < 0.01$, analysis of variance, measured *versus* vehicle-treated, NP-OVA-immunized mice, except where indicated by *brackets*). As each slide had only some sections of the spleen, the actual number of GCs per mouse would be proportionally higher.

BCR signaling is to promote Ca^{2+} mobilization and suggests that maximal AKT activity is not required to sustain B cell proliferation in response to antigen.

Our data indicate that the p110δ inhibitor IC87114 suppresses B cell survival in response to anti-IgM or BAFF, but to a lesser extent than the more broad-spectrum PI3K inhibitor GDC-0941. The finding that GDC-0941 has cytotoxic effects on B cells *in vitro* is consistent with the observation of Ramadani *et al.* (20) that inactivation of both p110α and p110δ causes a nearly complete loss of mature B cells *in vivo*. The apparent redundancy of p110α and p110δ in supporting B cell survival is noteworthy in light of the clinical success of the investigational

agent CAL-101 (now GS-1101). This selective p110δ inhibitor has shown impressive efficacy in human patients with chronic lymphocytic leukemia, yet its primary mechanism of action seems to be disruption of the tumor microenvironment rather than direct cytotoxic effects on malignant B cells (3). It is possible that a combined inhibitor of p110α and p110δ would have more potent anti-tumor effects in chronic lymphocytic leukemia and other lymphoid malignancies.

Disruption of the MZ B cell subset is now recognized as a biomarker of p110δ inhibition in mice (28, 40). Genetic studies in mice suggest that a central signaling pathway governing MZ B cell development is initiated by CD19 on the cell surface, which signals via PI3K-p110δ and AKT to suppress the transcription factor Foxo1 (40). Pharmacological inhibition of p110δ using IC87114 reduces MZ B cell numbers but also disrupts their localization, with IgM^{hi}/IgD^{lo} B cells moving into the follicles (28). This is consistent with other data showing that chemokine responses in MZ B cells are largely dependent on the p110δ isoform (28). We confirmed that IC87114 suppresses AKT phosphorylation induced in B cells by the chemokine CXCL13, to a greater extent than in cells treated with p110α or p110β inhibitors (data not shown).

The p110δ isoform has important functions in T cell clonal expansion, differentiation, and trafficking (16). However, PI3K activation is not fully abrogated in p110δ-deficient T cells and some functional capacity is retained (38). It is likely, therefore, that other PI3K catalytic isoforms contribute to T cell function. Some studies have suggested that the class IB isoform p110γ has overlapping functions in T cells, whereas others have disputed this claim (16). In this study we focused on class IA isoforms, in part because available inhibitors are not sufficiently selective for p110γ. Using antigen-specific mouse T cells and PHA-activated human T cells, we found that proliferative expansion is not significantly reduced by selective inhibition of individual class IA isoforms. Moreover, the pan-class I inhibitors suppressed T cell proliferation to a greater extent than the combination of IC87114 and MLN1316. Together these findings suggest that all four class I isoforms might be engaged during the course of antigen-specific T cell activation. Interesting questions to resolve are whether the isoforms act downstream of different receptors (*i.e.* TCR, costimulatory, cytokine, chemokine receptors) and whether they function in a temporal order.

An apparent paradox in our data is the observation that GDC-0941 and IC87114 suppress formation of germinal centers yet they have no effect on titers of high affinity, class-switched antibodies whose production is thought to be dependent on the germinal center reaction. The absence of GCs in IC87114-treated mice is consistent with previous work identifying a specific role for p110δ in the differentiation and function of T follicular-helper (Tfh) cells, a subset of CD4 T cells required for GC formation (41). In addition, our data on NP-specific Ig production agree with previous studies showing that IC87114 does not impair class-switched antibody responses in mice (39). Indeed, p110δ inhibition enhances IgE production (39), a finding reproduced here. One possibility is that an extrafollicular (non-GC-based) B cell response that is Tfh-independent might be sufficient to produce antigen-specific antibody responses to protein antigens in mice treated with IC87114 or GDC-0941. Regardless, a key point is that p110α inhibition using MLN1117 *in vivo* has no measurable effect on antibody responses or GC formation. This suggests that p110α is not required for Tfh differentiation or help to B cells in general.

Many years of medicinal chemistry efforts have resulted in an expanded toolkit for probing the function of specific PI3K catalytic isoforms (42). In this study we set out to determine how selective inhibitors of p110α impact the function of T and B cells, key components of the adaptive immune system. The most important conclusion is that p110α inhibition does not significantly impair mouse and human lymphocyte proliferation *in vitro*, nor antibody responses *in vivo*, at doses demonstrating potent anti-tumor activity in preclinical models. A key implication is that selective p110α inhibitors that are in clinical trials for cancer are likely to be less immunosuppressive than pan-class I or p110δ-selective agents. The combined p110α/β inhibitor MLN1316 also had only modest effects on lymphocyte function, suggesting that anti-cancer compounds with this profile would likewise show minimal immunosuppression. Our results do not rule out the possibility that p110α and/or p110β inhibition can modulate lymphocyte differentiation and effector function in certain contexts. This possibility warrants further investigation using the growing assortment of PI3K isoform-selective compounds. Compounds targeting two isoforms (*e.g.* p110α/δ and p110γ/δ) might also have unique effects in lymphocytes. The ability of PI3K inhibitors to enhance innate immune responses (43) also requires further investigation. A better understanding of PI3K isoforms in the immune system will improve our ability to predict and manage immunosuppression and to potentially manipulate the immune components of the tumor microenvironment.

Acknowledgments—We thank Elizabeth Clarke and Andrea Tenner for providing human T cells, and Jack Xu and Paolo Casali for help with human B cell experiments.

REFERENCES

1. Vanhaesebroeck, B., Guillermet-Guibert, J., Graupera, M., and Bilanges, B. (2010) The emerging mechanisms of isoform-specific PI3K signalling. *Nat. Rev. Mol. Cell Biol.* **11,** 329–341
2. Agarwal, R., Carey, M., Hennessy, B., and Mills, G. B. (2010) PI3K pathway-directed therapeutic strategies in cancer. *Curr. Opin. Investig. Drugs* **11,** 615–628
3. Fruman, D. A., and Rommel, C. (2011) PI3Kδ inhibitors in cancer. Rationale and serendipity merge in the clinic. *Cancer Discov.* **1,** 562–572
4. Hanahan, D., and Weinberg, R. A. (2011) Hallmarks of cancer: the next generation. *Cell* **144,** 646–674
5. Wong, K. K., Engelman, J. A., and Cantley, L. C. (2010) Targeting the PI3K signaling pathway in cancer. *Curr. Opin. Gen. Dev.* **20,** 87–90
6. Samuels, Y., Wang, Z., Bardelli, A., Silliman, N., Ptak, J., Szabo, S., Yan, H., Gazdar, A., Powell, S. M., Riggins, G. J., Willson, J. K., Markowitz, S., Kinzler, K. W., Vogelstein, B., and Velculescu, V. E. (2004) High frequency of mutations of the *PIK3CA* gene in human cancers. *Science* **304,** 554
7. Engelman, J. A., Chen, L., Tan, X., Crosby, K., Guimaraes, A. R., Upadhyay, R., Maira, M., McNamara, K., Perera, S. A., Song, Y., Chirieac, L. R., Kaur, R., Lightbown, A., Simendinger, J., Li, T., Padera, R. F., García-Echeverría, C., Weissleder, R., Mahmood, U., Cantley, L. C., and Wong, K. K. (2008) Effective use of PI3K and MEK inhibitors to treat mutant Kras G12D and PIK3CA H1047R murine lung cancers. *Nat. Med.* **14,** 1351–1356
8. Liu, P., Cheng, H., Santiago, S., Raeder, M., Zhang, F., Isabella, A., Yang, J.,

Semaan, D. J., Chen, C., Fox, E. A., Gray, N. S., Monahan, J., Schlegel, R., Beroukhim, R., Mills, G. B., and Zhao, J. J. (2011) Oncogenic PIK3CA-driven mammary tumors frequently recur via PI3K pathway-dependent and PI3K pathway-independent mechanisms. *Nat. Med.* **17,** 1116–1120

9. Jamieson, S., Flanagan, J. U., Kolekar, S., Buchanan, C., Kendall, J. D., Lee, W. J., Rewcastle, G. W., Denny, W. A., Singh, R., Dickson, J., Baguley, B. C., and Shepherd, P. R. (2011) A drug targeting only p110α can block phosphoinositide 3-kinase signalling and tumour growth in certain cell types. *Biochem. J.* **438,** 53–62
10. O'Brien, C., Wallin, J. J., Sampath, D., GuhaThakurta, D., Savage, H., Punnoose, E. A., Guan, J., Berry, L., Prior, W. W., Amler, L. C., Belvin, M., Friedman, L. S., and Lackner, M. R. (2010) Predictive biomarkers of sensitivity to the phosphatidylinositol 3′-kinase inhibitor GDC-0941 in breast cancer preclinical models. *Clin. Cancer Res.* **16,** 3670–3683
11. Edgar, K. A., Wallin, J. J., Berry, M., Lee, L. B., Prior, W. W., Sampath, D., Friedman, L. S., and Belvin, M. (2010) Isoform-specific phosphoinositide 3-kinase inhibitors exert distinct effects in solid tumors. *Cancer Res.* **70,** 1164–1172
12. Jia, S., Liu, Z., Zhang, S., Liu, P., Zhang, L., Lee, S. H., Zhang, J., Signoretti, S., Loda, M., Roberts, T. M., and Zhao, J. J. (2008) Essential roles of PI(3)K-p110β in cell growth, metabolism and tumorigenesis. *Nature* **454,** 776–779
13. Deleted in proof
14. Rakhra, K., Bachireddy, P., Zabuawala, T., Zeiser, R., Xu, L., Kopelman, A., Fan, A. C., Yang, Q., Braunstein, L., Crosby, E., Ryeom, S., and Felsher, D. W. (2010) $CD4^+$ T cells contribute to the remodeling of the microenvironment required for sustained tumor regression upon oncogene inactivation. *Cancer Cell* **18,** 485–498
15. Vanneman, M., and Dranoff, G. (2012) Combining immunotherapy and targeted therapies in cancer treatment. *Nat. Rev. Cancer* **12,** 237–251
16. Okkenhaug, K., and Fruman, D. A. (2010) PI3Ks in lymphocyte signaling and development. *Curr. Top. Microbiol. Immunol.* **346,** 57–85
17. Bi, L., Okabe, I., Bernard, D. J., Wynshaw-Boris, A., and Nussbaum, R. L. (1999) Proliferative defect and embryonic lethality in mice homozygous for a deletion in the p110α subunit of phosphoinositide 3-kinase. *J. Biol. Chem.* **274,** 10963–10968
18. Foukas, L. C., Claret, M., Pearce, W., Okkenhaug, K., Meek, S., Peskett, E., Sancho, S., Smith, A. J., Withers, D. J., and Vanhaesebroeck, B. (2006) Critical role for the p110α phosphoinositide-3-OH kinase in growth and metabolic regulation. *Nature* **441,** 366–370
19. Graupera, M., Guillermet-Guibert, J., Foukas, L. C., Phng, L. K., Cain, R. J., Salpekar, A., Pearce, W., Meek, S., Millan, J., Cutillas, P. R., Smith, A. J., Ridley, A. J., Ruhrberg, C., Gerhardt, H., and Vanhaesebroeck, B. (2008) Angiogenesis selectively requires the p110α isoform of PI3K to control endothelial cell migration. *Nature* **453,** 662–666
20. Ramadani, F., Bolland, D. J., Garcon, F., Emery, J. L., Vanhaesebroeck, B., Corcoran, A. E., and Okkenhaug, K. (2010) The PI3K isoforms p110α and p110δ are essential for pre-B cell receptor signaling and B cell development. *Sci. Signal* **3,** ra60
21. Janes, M. R., Limon, J. J., So, L., Chen, J., Lim, R. J., Chavez, M. A., Vu, C., Lilly, M. B., Mallya, S., Ong, S. T., Konopleva, M., Martin, M. B., Ren, P., Liu, Y., Rommel, C., and Fruman, D. A. (2010) Effective and selective targeting of leukemia cells using a TORC1/2 kinase inhibitor. *Nat. Med.* **16,** 205–213
22. Donahue, A. C., and Fruman, D. A. (2007) Distinct signaling mechanisms activate the target of rapamycin in response to different B-cell stimuli. *Eur. J. Immunol.* **37,** 2923–2936
23. Sun, M., Hillmann, P., Hofmann, B. T., Hart, J. R., and Vogt, P. K. (2010) Cancer-derived mutations in the regulatory subunit p85α of phosphoinositide 3-kinase function through the catalytic subunit p110α. *Proc. Natl. Acad. Sci. U.S.A.* **107,** 15547–15552
24. Jessen, K., Kessler, L., Kucharski, J., Guo, X., Staunton, J., Janes, M. R., Elia, M., Banerjee, U., Lan, L., Wang, S., Stewart, J., Luzader, A., Darjania, L., Li, L., Chan, K., Martin, M., Ren, P., Rommel, C., and Liu, Y. (2011) A potent and selective PI3K inhibitor, INK1117, targets human cancers harboring oncogenic PIK3CA mutations. *Mol. Cancer Ther.* **10,** Abstr. A171
25. Chaussade, C., Rewcastle, G. W., Kendall, J. D., Denny, W. A., Cho, K., Grønning, L. M., Chong, M. L., Anagnostou, S. H., Jackson, S. P., Daniele, N., and Shepherd, P. R. (2007) Evidence for functional redundancy of class IA PI3K isoforms in insulin signalling. *Biochem. J.* **404,** 449–458
26. Jackson, S. P., Schoenwaelder, S. M., Goncalves, I., Nesbitt, W. S., Yap, C. L., Wright, C. E., Kenche, V., Anderson, K. E., Dopheide, S. M., Yuan, Y., Sturgeon, S. A., Prabaharan, H., Thompson, P. E., Smith, G. D., Shepherd, P. R., Daniele, N., Kulkarni, S., Abbott, B., Saylik, D., Jones, C., Lu, L., Giuliano, S., Hughan, S. C., Angus, J. A., Robertson, A. D., and Salem, H. H. (2005) PI 3-kinase p110β. A new target for antithrombotic therapy. *Nat. Med.* **11,** 507–514
27. Bilancio, A., Okkenhaug, K., Camps, M., Emery, J. L., Ruckle, T., Rommel, C., and Vanhaesebroeck, B. (2006) Key role of the p110δ isoform of PI3K in B-cell antigen and IL-4 receptor signaling. Comparative analysis of genetic and pharmacologic interference with p110δ function in B cells. *Blood* **107,** 642–650
28. Durand, C. A., Hartvigsen, K., Fogelstrand, L., Kim, S., Iritani, S., Vanhaesebroeck, B., Witztum, J. L., Puri, K. D., and Gold, M. R. (2009) Phosphoinositide 3-kinase p110δ regulates natural antibody production, marginal zone and B-1 B cell function, and autoantibody responses. *J. Immunol.* **183,** 5673–5684
29. Soond, D. R., Bjørgo, E., Moltu, K., Dale, V. Q., Patton, D. T., Torgersen, K. M., Galleway, F., Twomey, B., Clark, J., Gaston, J. S., Taskén, K., Bunyard, P., and Okkenhaug, K. (2010) PI3K p110δ regulates T-cell cytokine production during primary and secondary immune responses in mice and humans. *Blood* **115,** 2203–2213
30. Folkes, A. J., Ahmadi, K., Alderton, W. K., Alix, S., Baker, S. J., Box, G., Chuckowree, I. S., Clarke, P. A., Depledge, P., Eccles, S. A., Friedman, L. S., Hayes, A., Hancox, T. C., Kugendradas, A., Lensun, L., Moore, P., Olivero, A. G., Pang, J., Patel, S., Pergl-Wilson, G. H., Raynaud, F. I., Robson, A., Saghir, N., Salphati, L., Sohal, S., Ultsch, M. H., Valenti, M., Wallweber, H. J., Wan, N. C., Wiesmann, C., Workman, P., Zhyvoloup, A., Zvelebil, M. J., and Shuttleworth, S. J. (2008) The identification of 2-(1H-indazol-4-yl)-6-(4-methanesulfonyl-piperazin-1-yl-methyl)-4-morpholine-4-yl-thieno[3,2-*d*]pyrimidine (GDC-0941) as a potent, selective, orally bioavailable inhibitor of class I PI3 kinase for the treatment of cancer. *J. Med. Chem.* **51,** 5522–5532
31. Raynaud, F. I., Eccles, S. A., Patel, S., Alix, S., Box, G., Chuckowree, I., Folkes, A., Gowan, S., De Haven Brandon, A., Di Stefano, F., Hayes, A., Henley, A. T., Lensun, L., Pergl-Wilson, G., Robson, A., Saghir, N., Zhyvoloup, A., McDonald, E., Sheldrake, P., Shuttleworth, S., Valenti, M., Wan, N. C., Clarke, P. A., and Workman, P. (2009) Biological properties of potent inhibitors of class I phosphatidylinositide 3-kinases. From PI-103 through PI-540, PI-620 to the oral agent GDC-0941. *Mol. Cancer Ther.* **8,** 1725–1738
32. Kong, D., and Yamori, T. (2007) ZSTK474 is an ATP-competitive inhibitor of class I phosphatidylinositol 3-kinase isoforms. *Cancer Sci.* **98,** 1638–1642
33. Rewcastle, G. W., Gamage, S. A., Flanagan, J. U., Frederick, R., Denny, W. A., Baguley, B. C., Kestell, P., Singh, R., Kendall, J. D., Marshall, E. S., Lill, C. L., Lee, W. J., Kolekar, S., Buchanan, C. M., Jamieson, S. M., and Shepherd, P. R. (2011) Synthesis and biological evaluation of novel analogues of the pan class I phosphatidylinositol 3-kinase (PI3K) inhibitor 2-(difluoromethyl)-1-[4,6-di(4-morpholinyl)-1,3,5-triazin-2-yl]-1H-benzimidazole (ZSTK474). *J. Med. Chem.* **54,** 7105–7126
34. Wee, S., Wiederschain, D., Maira, S. M., Loo, A., Miller, C., deBeaumont, R., Stegmeier, F., Yao, Y. M., and Lengauer, C. (2008) PTEN-deficient cancers depend on PIK3CB. *Proc. Natl. Acad. Sci. U.S.A.* **105,** 13057–13062
35. Okkenhaug, K., Ali, K., and Vanhaesebroeck, B. (2007) Antigen receptor signalling. A distinctive role for the p110δ isoform of PI3K. *Trends Immunol.* **28,** 80–87
36. Fruman, D. A., Satterthwaite, A. B., and Witte, O. N. (2000) Xid-like phenotypes. A B cell signalosome takes shape. *Immunity* **13,** 1–3
37. Okkenhaug, K., Bilancio, A., Farjot, G., Priddle, H., Sancho, S., Peskett, E., Pearce, W., Meek, S. E., Salpekar, A., Waterfield, M. D., Smith, A. J., and Vanhaesebroeck, B. (2002) Impaired B and T cell antigen receptor signaling in p110δ PI 3-kinase mutant mice. *Science* **297,** 1031–1034
38. Okkenhaug, K., Patton, D. T., Bilancio, A., Garçon, F., Rowan, W. C., and Vanhaesebroeck, B. (2006) The p110δ isoform of phosphoinositide 3-ki-

nase controls clonal expansion and differentiation of Th cells. *J. Immunol.* **177,** 5122–5128
39. Zhang, T. T., Okkenhaug, K., Nashed, B. F., Puri, K. D., Knight, Z. A., Shokat, K. M., Vanhaesebroeck, B., and Marshall, A. J. (2008) Genetic or pharmaceutical blockade of p110δ phosphoinositide 3-kinase enhances IgE production. *J. Allergy Clin. Immunol.* **122,** 811–819.e2
40. So, L., and Fruman, D. A. (2012) PI3K signalling in B- and T-lymphocytes. New developments and therapeutic advances. *Biochem. J.* **442,** 465–481
41. Rolf, J., Bell, S. E., Kovesdi, D., Janas, M. L., Soond, D. R., Webb, L. M., Santinelli, S., Saunders, T., Hebeis, B., Killeen, N., Okkenhaug, K., and Turner, M. (2010) Phosphoinositide 3-kinase activity in T cells regulates the magnitude of the germinal center reaction. *J. Immunol.* **185,** 4042–4052
42. Workman, P., Clarke, P. A., Raynaud, F. I., and van Montfort, R. L. (2010) Drugging the PI3 kinome. From chemical tools to drugs in the clinic. *Cancer Res.* **70,** 2146–2157
43. Marshall, N. A., Galvin, K. C., Corcoran, A. M., Boon, L., Higgs, R., and Mills, K. H. (2012) Immunotherapy with PI3K inhibitor and Toll-like receptor agonist induces IFN-γ+IL-17+ polyfunctional T cells that mediate rejection of murine tumors. *Cancer Res.* **72,** 581–591